Original scientific paper

Synthesis of CuInSe$_2$ thin films from electrodeposited Cu$_{11}$In$_9$ precursors by two-step annealing

TSUNG-WEI CHANG, SHAO-YU HU, WEN-HSI LEE$^{\boxtimes}$

Department of Electrical Engineering, National Cheng Kung University, Tainan 701, Taiwan, R.O.C

$^{\boxtimes}$Corresponding Authors: E-mail: leewen@mail.ncku.edu.tw

Abstract

In this study, copper indium selenide (CIS) films were synthesized from electrodeposited Cu-In-Se precursors by two-step annealing. The agglomeration phenomenon of the electrodeposited In layer usually occurred on the Cu surface. A thermal process was adopted to turn Cu-In precursors into uniform Cu$_{11}$In$_9$ binary compounds. After deposition of the Se layer, annealing was employed to form chalcopyrite CIS. However, synthesis of CIS from Cu$_{11}$In$_9$ requires sufficient thermal energy. Annealing temperature and time were investigated to grow high quality CIS film. Various electrodeposition conditions were investigated to achieve the proper atomic ratio of CIS. The properties of the CIS films were characterized by scanning electron microscopy (SEM), X-ray Diffraction (XRD), and Raman spectra.

Keywords

CuInSe$_2$, CIS, Annealing, Electrodeposition

Introduction

The solar cell has emerged as a very important non-conventional energy source. Copper indium selenide (CuInSe$_2$) is a I–III–VI group semiconductor compound offering good possibilities for thin-film photovoltaic (PV) applications because it has a energy gap of 1.02 eV [1–5]. Electrochemical deposition is a low cost method of producing thin CIS films because it has several advantages for large-area non-vacuum thin film production and little material waste. However, the crystallinity of CIS film grown by single-step electrodeposition is inferior because its growing temperature is much lower than that of the physical vapour deposition (PVD) method. The grains were small and loose. The CIS film can also be synthesized from co-sputtered Cu$_{11}$In$_9$-Se precursors by the thermal annealing process [6,7]. Large CIS grains can be grown due to the gas–liquid reaction during the annealing process [8]. The Cu-In alloys are usually co-sputtered by PVD. The PVD technology is

excellent for good quality film growth but difficult to scale up because of the high manufacturing costs.

In this study, Cu-In precursors were prepared by multi-step electrodeposition. However, the agglomeration phenomenon of the electrodeposited In layer usually occurred on the Cu surface. The surface was non-uniform and discontinuous. An annealing process was adopted to transform Cu-In to Cu$_{11}$In$_9$ compound and create a uniform surface structure. After deposition of the Se layer on the annealed Cu$_{11}$In$_9$, another annealing process is required to synthesize the CIS structure. Various annealing temperatures and times were adopted to investigate the proper annealing conditions and the mechanism of CIS synthesis. The deposition conditions were adjusted to achieve a better atomic ratio. The properties of the CIS films were characterized by scanning electron microscopy (SEM), X-ray Diffraction (XRD), and Raman spectra.

Experiment

The aqueous solution for the Cu deposition contained 0.75 M CuSO$_4$, 4 mM H$_2$SO$_4$, and 0.5 mM HCl. The aqueous solution for the Se deposition contained 17 mM H$_2$SeO$_3$ and 0.5 mM HCl. The aqueous solution for the In deposition contained 50 mM InCl$_3$ and 30 mM HCl. The electrodepositions were carried out with AUTOLAB PGSTAT302, a conventional three-electrode potentiostat, and the deposition conditions listed in Table 1. A thin slice of 99.99% pure Pt electrode measuring 1×4 cm was employed as the counter electrode, and an Ag/AgCl electrode served as the reference electrode. Glass substrates with sputtered Mo film were used as the working electrodes. The electrodeposition area was a square measuring 1 x 1 cm. The substrates were cleaned by ultrasonication in acetone, 99.5 % pure ethanol, and water before sputtering and electrodeposition. A magnetic stirrer was used for the stirring procedure. The rotation speed of the magnetic stirrer was set at 50 rpm.

Table 1. Electrodeposition and annealing condition of samples a - f.

	Cu	**In**	**Se**		$T_{annealing}$ / °C
	i / mA : τ / s	τ / s (i = 5 mA)	i / mA	τ / s	(τ = 5 min)
Sample a	60 : 20 + 20 : 10	350	4	1450	550
Sample b	60 : 20 + 20 : 10	350	4	1450	600
Sample c	60 : 20 + 20 : 10	350	4	1450	650
Sample d	70 : 20 + 20 : 10	350	4	1450	650
Sample e	60 : 10 + 30 : 10	375	4	1450	650
Sample f	50 : 10 + 20 : 10	350	4	1450	650

The In deposition was carried out after the two-step growth of Cu. The Cu-In layers were treated by rapid thermal annealing (RTA) at 500 °C for 5 min. The Se layer was deposited on the Cu-In layer after annealing. The CIS film was synthesized by annealing the Cu-Se and In-Se precursors. The deposition conditions and RTA listed in Table 1 were found to achieve better proportions and structures.

The surface morphology and chemical composition of the films were characterized by SEM (Philips XL-40FEG) and EDS, respectively. The Raman spectra were produced with a backscattering configuration at room temperature with unpolarized light using a DILOR XY 800 spectrometer and

an Ar laser with a 514.5 nm wavelength as the light source. The phase composition and the crystallographic structure were analysed by XRD using a Bruker D8 SSS multipurpose thin-film x-ray diffractometer.

Results and discussion

In this study, $CuInSe_2$ thin films were synthesized from electrodeposited Cu, In, and Se thin-film precursors. However, the electrodeposition of the In layer on the copper surface with a current of 60 mA in 20 s + 20 mA in 10 s induced serious agglomeration phenomenon. Figure 1 shows the SEM image of the deposited In on the Cu layer. It was deposited with a current density of 3-6 mA cm^{-2}. The agglomeration phenomenon made it difficult for the In layer to cover the whole surface. The grains of In were separated. Deposition with a high current density can lead to a better distribution of In. However, it also leads to large over potential, which would cause bubbles and a rough structure. A suitable value of 5 mA was employed for the deposition of In. After the deposition of Se, the Cu-In-Se precursor was annealed by RTA to form the CIS structure. The XRD results in Figure 2 show that the CIS structure can be synthesized at 450-550 °C. However, the SEM images in Figure 3 show that the film has a rough surface and a non-uniform grain size. The CIS structure came from the non-uniform In layer and the miscellaneous precursor type. The precursors not only contain Cu, In and Se, but also some binary compounds, including $Cu_{11}In_9$, Cu_xSe and In_2Se_3, which were produced in the electrodeposition and annealing process. Different precursors have different reactions and temperature requirements to form CIS, and other reactions lead to a uniform structure [9].
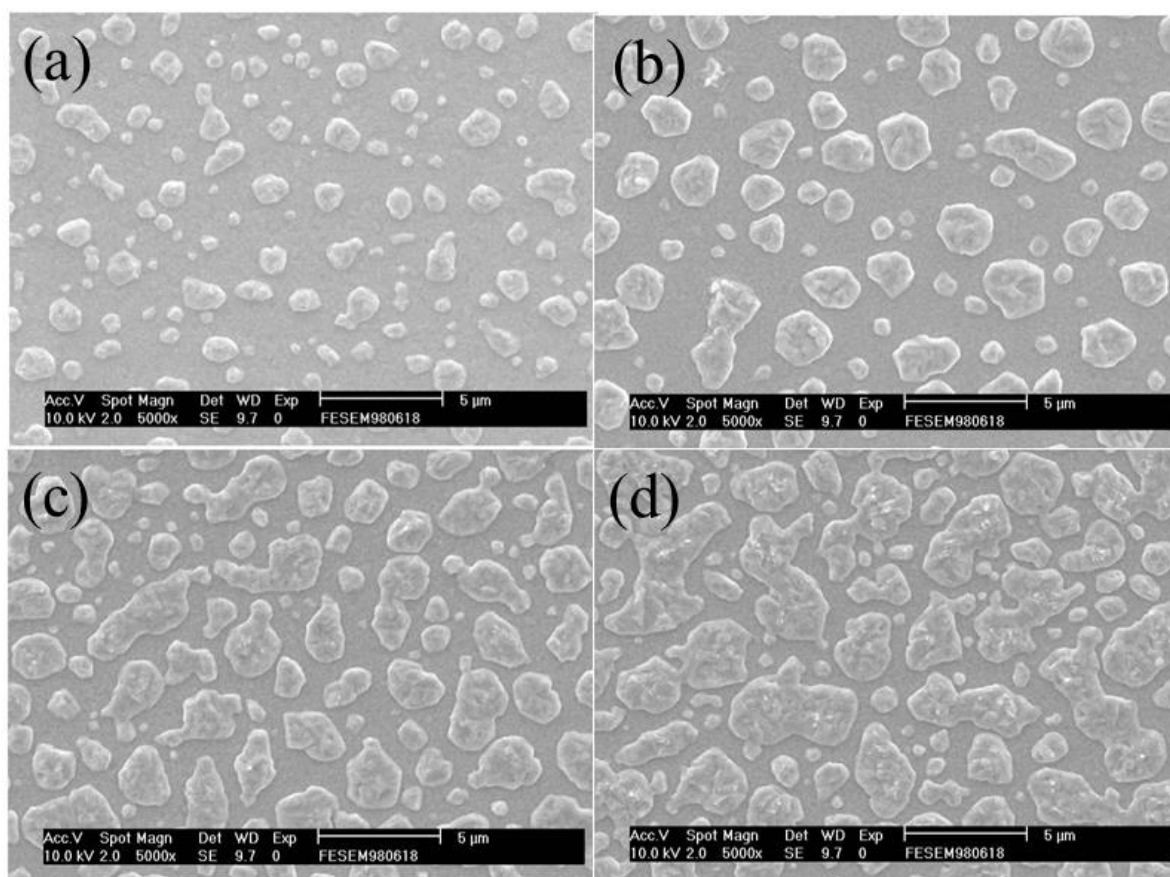

Fig. 1. *SEM images of deposited In on Cu surface with current densities (a) 3 mA cm^{-2} (b) 4 mA cm^{-2} (c) 5 mA cm^{-2} (d) 6 mA cm^{-2} for 200s.*
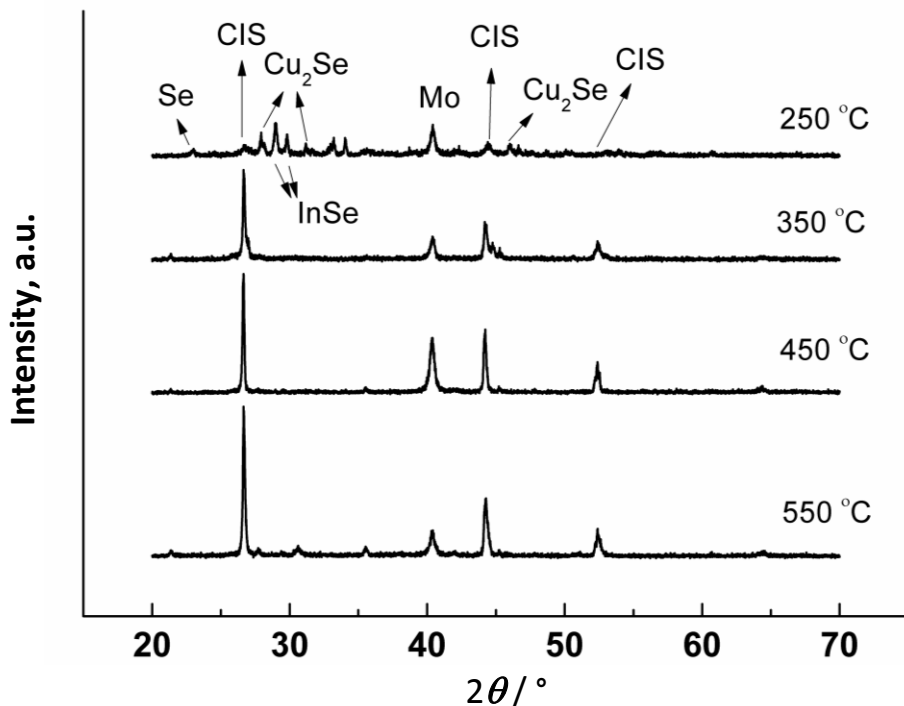
Fig. 2. *XRD of annealed CIS film synthesized from Cu-In-Se precursor with temperature.*
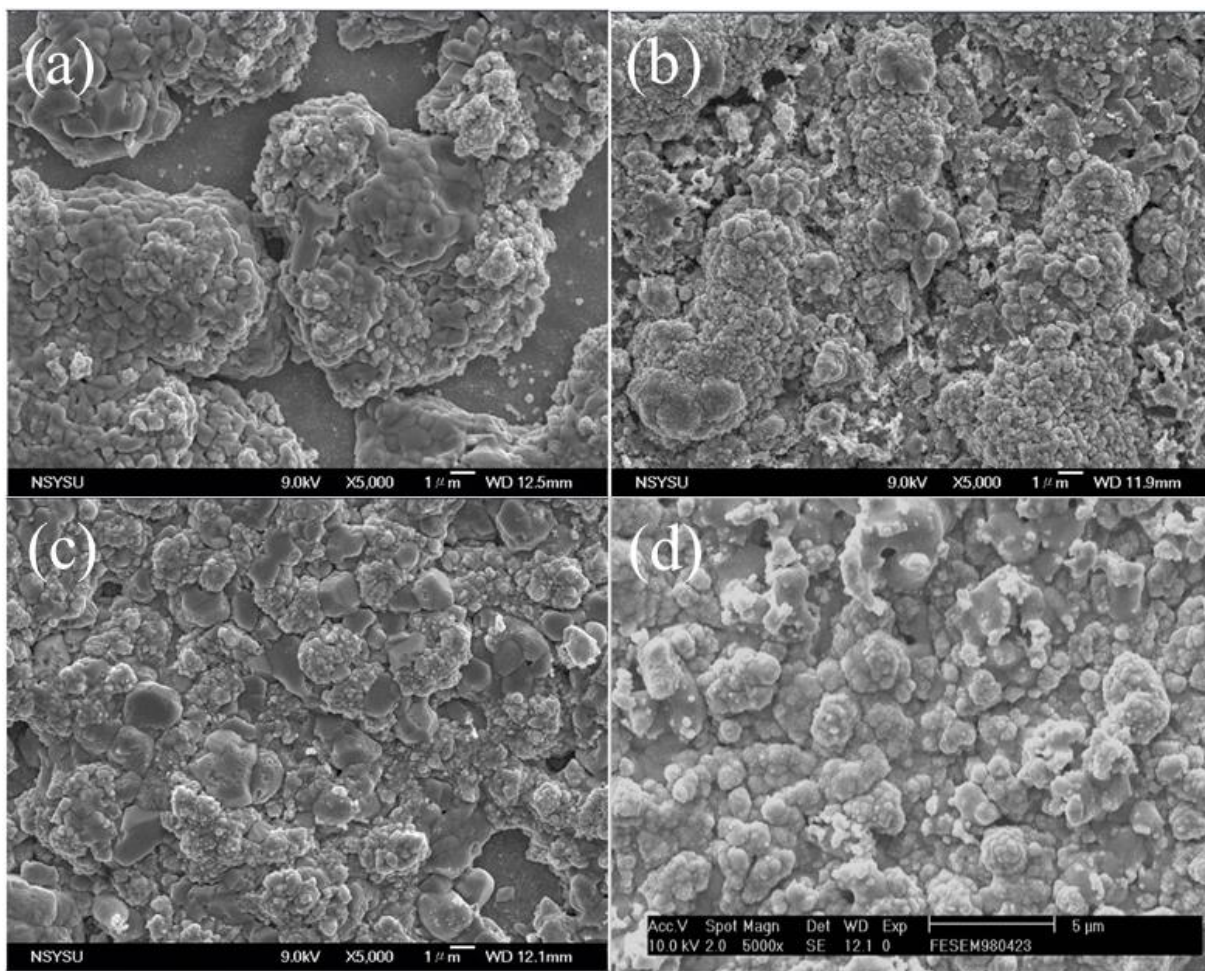

Fig. 3. *SEM images of annealed CIS film synthesized from bilayer electrodeposition of Cu-In-Se precursors with temperature (a) 250 °C, (b) 350 °C, (c) 450 °C, (d) 550 °C.*

In order to create a smooth In layer distribution and uniform CIS synthesis, a thermal pre-treatment at 500 °C for 5 min was employed to improve the topography of the Cu-In layer. Figure 4 shows the SEM image of the Cu-In thin film after annealing at 500 °C for 5 min. The film re-grows continuously and covers the whole Cu surface. Figure 5 shows the XRD pattern of the annealed Cu-In precursor. Most of the precursors were turned to $Cu_{11}In_9$ and small amounts to $CuInSe_2$.
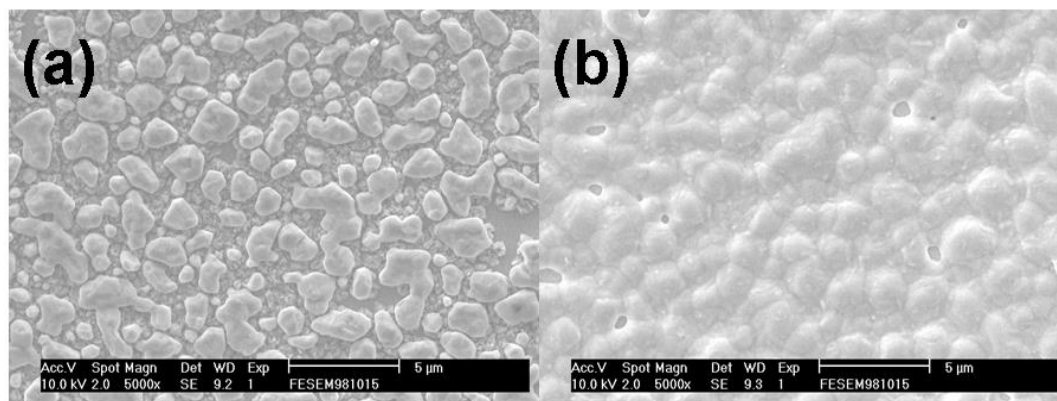

Fig. 4. *SEM images of electrodeposited In layer on Cu surface (a) as-deposited film (b) annealed film.*
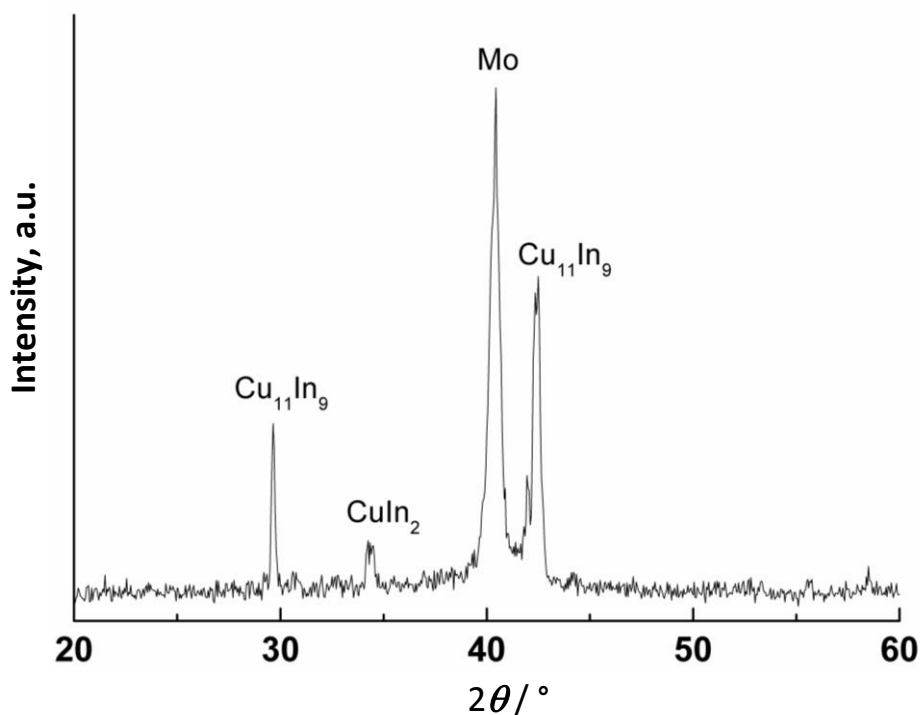

Fig.5. *XRD pattern of annealed Cu/In precursors.*

The Se layer was deposited on the annealed Cu-In surface at 4 mA cm^{-2} current density for 1200 s. All of the precursors were recrystallized by RTA at 600 °C for 3 min and observed by SEM and EDS. Figure 6(a) shows the microstructure of the annealed CIS film at 600 °C for 3 min. The grain size of the annealed CIS film synthesized from $Cu_{11}In_9$-Se precursors is much larger than that of CIS film annealed by co-electrodeposition. During the thermal annealing, the Cu-In became liquid phase and reacted with the gas phase Se. CIS grain growing and diffusion were easier in the gas-liquid reaction. However, many voids were observed in the SEM image. This was because CIS synthesis from the reaction of $Cu_{11}In_9$-Se precursors requires a higher annealing temperature.

Figure 6(b) shows the microstructure of the CIS film with an annealing temperature of 630 °C for 3 min. A higher synthesis temperature certainly reduces the voids in the film.

However, the EDS results shown in Table 2 indicate that the composition of the film is not optimum for CIS. Se gas would easily dissipate during annealing. In Samples a, b, and c listed in Table 1, the deposition times of Se was increased to 1450 s and the annealing temperature was adjusted to find the proper value. The EDS results shown in Table 2 indicate that the atomic ratio of Se increases to an appropriate value of 50 %.
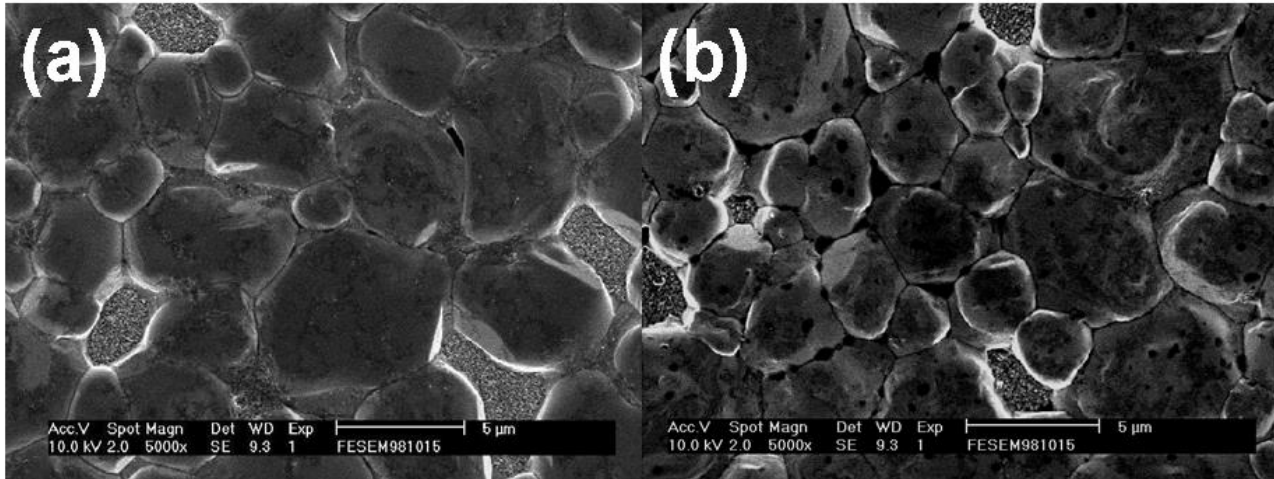

Fig. 6. *SEM images of CIS film after annealing at (a) 600 °C, (b) 630°C for 3min.*

Table 2. *The EDS analysis of atomic percent of CIS film after increasing the deposition time for 1200 s and 1450 s of Se*

at. % of Cu	at. % of In	at. % of Se	Cu/In ratio	Se deposition time, s
29.1	24.7	46.2	1.17	1200
26.6	23.2	50.2	1.14	1450

Figure 7 shows the SEM images of Samples a, b, and c. It is observed that increasing the annealing temperature can increase the grain size of the CIS film. The voids on the surface were also reduced with the higher temperature. A higher annealing temperature could provide sufficient energy for the CIS film to diffuse and react more completely. The deposition condition was adjusted in Samples d, e, and f to achieve a proper Cu-In ratio. The EDS results are shown in Table 3. The Cu-In ratio of Sample f achieved nearly 1:1.
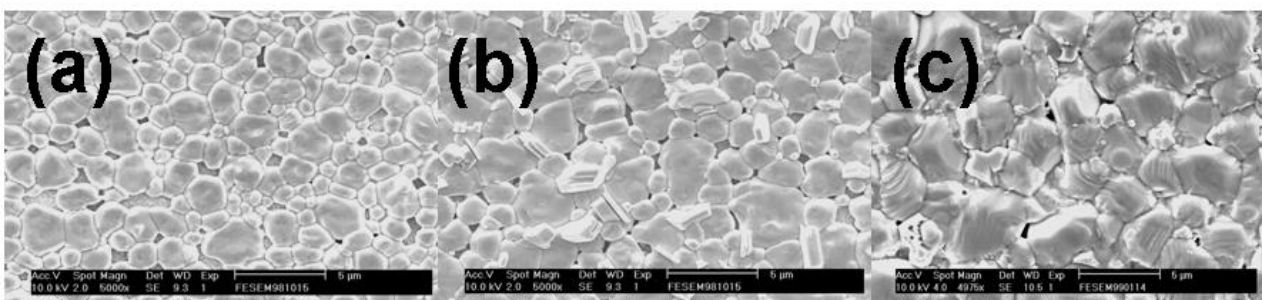

Fig. 7. *SEM images of CIS film with the Se layer deposited on the annealed Cu/In surface at 4 mA cm⁻² current density for 1200 s after annealing at (a) 600 °C (b) 630°C for 3min.*

Table 3. *The EDS analysis of atomic percent in samples d, e, and f.*

	at. % of Cu	at. % of In	at. % of Se	Cu/In ratio
Sample d	25.6	24.3	50.1	1.05
Sample e	25.4	22.8	51.8	1.11
Sample f	24.9	24.5	50.6	1.01

Figure 8 shows the SEM images of Sample f after annealing at 630 °C for 5 min and 10 min. The grain of CIS film became large and dense, and the voids almost disappear in Sample f. The cross-section images of Sample f are shown in Figure 9. Large dense grains could be clearly observed and the thickness of the CIS approached 2 μm.
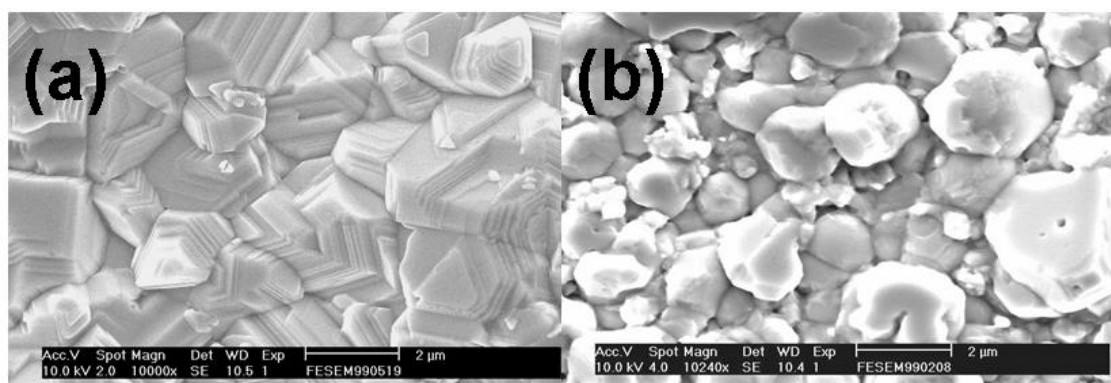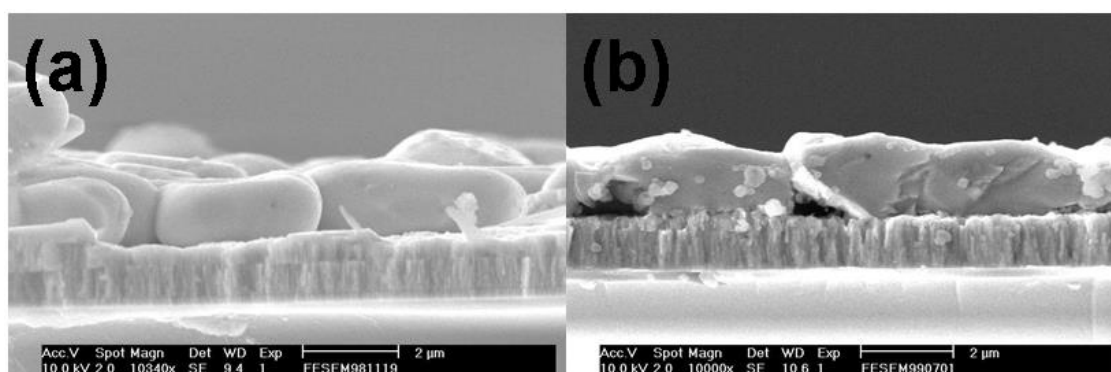

Fig. 8. *SEM images of sample f, annealed at 630 ℃ for (a) 5 min (b) 10 min.*

Fig. 9. *SEM images of cross-section of sample f, annealed at 630 °C for (a) 5 min, (b) 10 min.*

Figure 10 shows the XRD patterns of the CIS films with various annealing conditions. The main (112) peak confirmed the existence of chalcopyrite CIS. The (112) main peaks of the CIS films annealed at 550 °C for 5 min and at 600 °C for 5 min contained some small peaks of impure phase. However, the peaks were too close to be differentiated clearly by XRD, but the Raman analysis found $Cu_{1-x}Se_x$ or In_xSe.

A Raman spectrum was employed to analyse the film composition. Figure 11 shows the Raman spectra of the CIS films with various annealing conditions. Cu_2Se was found in the samples with the lower annealing temperature or shorter annealing time. This is because Cu_2Se was formed before the synthesis of CIS. If the annealing does not provide sufficient energy or reaction time, the precursors cannot completely transform to CIS. Figure 12 shows the XRD patterns of the CIS film with the lower annealing temperature. Cu-Se and In-Se were found at 300 °C and CIS (112) was found at 350 °C. This indicates that the precursors would turn into Cu-Se and In-Se binary compounds before the synthesis of the chalcopyrite CIS [10].
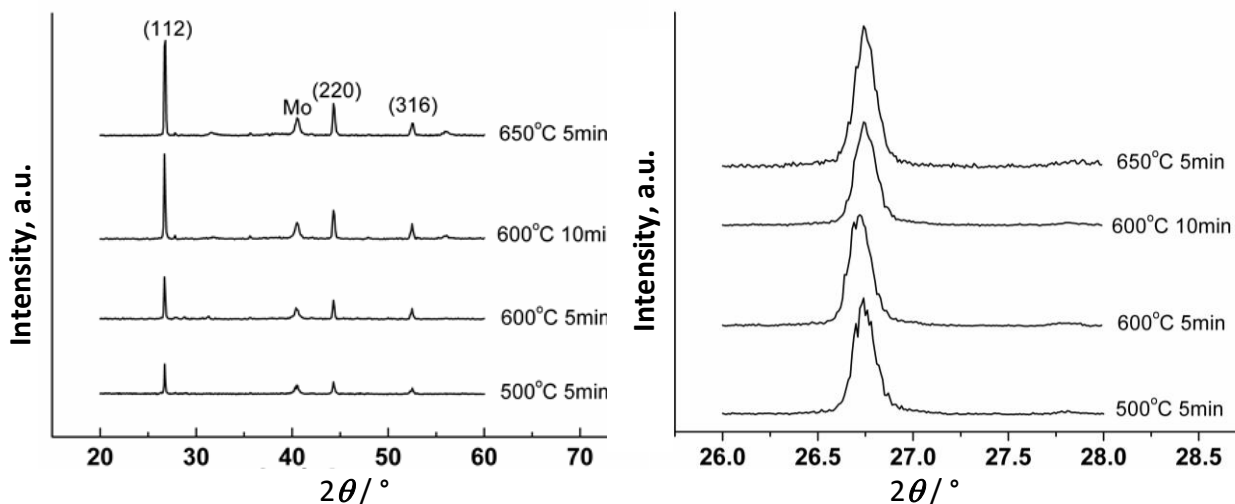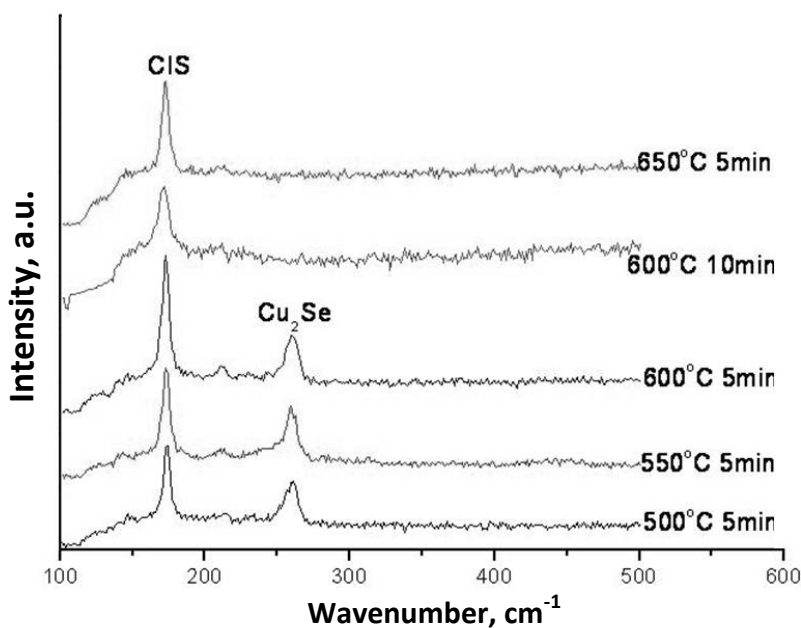
Fig.10. *XRD patterns of CIS films with conditions.*

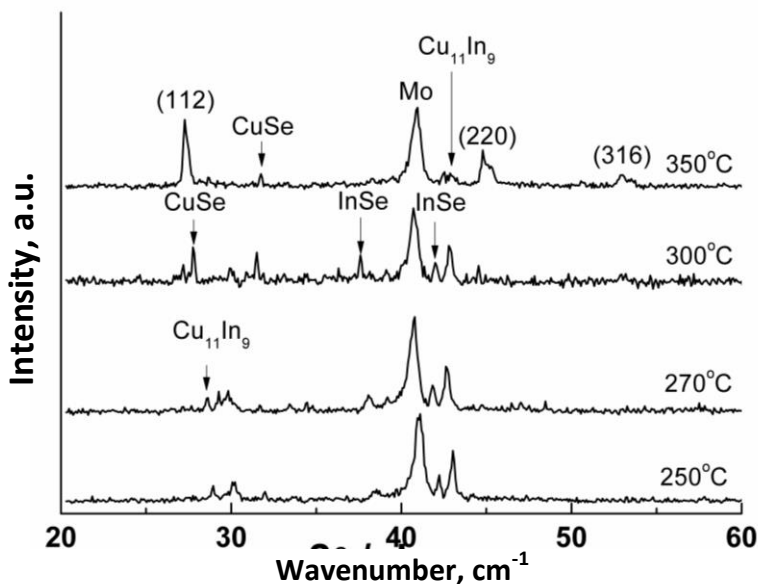**Fig.11.** *Raman spectra of CIS films obtained with conditions.*

Fig.12. *XRD patterns of CIS films after annealing at low temperature 250 ℃~350 ℃.*

However, synthesized CIS from co-sputtered $Cu_{11}In_9$ can produce high quality film with large grains. In this study, synthesis of the CIS from the electrodeposited Cu-In precursors was investigated. A thermal process was adopted to eliminate the agglomeration phenomenon of electrodeposited In and to form $Cu_{11}In_9$ compound. The electrodeposition conditions of Cu, In and Se, were adjusted to achieve the preferred atomic proportion. However, the annealing temperature of the synthesized CIS from $Cu_{11}In_9$ is critical. The XRD patterns and Raman spectra show that the residue of the Cu_2Se compound is due to an incomplete reaction at lower annealing temperatures. Large dense grains could be grown at 650 °C for 5 min. Finally, we produced a high quality CIS film with large grains from a cheap method of electrodeposition of Cu-In precursors.

Conclusions

Electrodeposition is a cheap and efficient method of producing CIS film. The crystallinity of the co-electrodeposited film is inferior because of the low growing temperature. Synthesizing CIS from co-sputtered $Cu_{11}In_9$ can produce high quality film with large grains. In this study, synthesizing CIS from electrodeposited Cu-In precursors was investigated. A thermal process was adopted to eliminate the agglomeration phenomenon of electrodeposited In to form $Cu_{11}In_9$ compound. The electrodeposition conditions of Cu, In and Se, were adjusted to achieve the preferred atomic proportion. However, the annealing temperature of synthesized CIS from $Cu_{11}In_9$ is critical. The XRD patterns and Raman spectra show that the Cu_2Se compound residue is due to an incomplete reaction at lower annealing temperatures. Large dense grains could be grown at 650 °C for 5 min.

References

[1]   K. Siemer, J. Klaer, I. Luck, J. Bruns, R. Klenk, D. Bräunig, *Sol. Energy Mater. Sol. Cells* **67** (2001) 159.
[2]   J. Klaer, I. Luck, A. Boden, R. Klenk, I. Gavilanes Perez, R. Scheer, *Thin Solid Films* **432** (2003) 534.
[3]   D. Lincot, J. F. Guillemoles, S. Taunier, D. Guimard, J. Sicx-Kurdi, A. Chaumont, O. Roussel, O. Ramdani, C. Hubert, J. P. Fauvarque, *Sol. Energy* **77** (2004) 725.
[4]   R. N. Bhattacharya, J. F. Hiltner, W. Batchelor, M. A. Contreras, R. N. Noufi, J. R. Sites, *Thin Solid Films* **361** (2000) 396.
[5]   K. Singh, R. Tanveer, *Sol. Energy Mater. Sol. Cells* **36** (1995) 409.
[6]   F.O. Adurodija, J. Song, S.D. Kim, S.H. Kwon, S.K. Kim, S.H. Yoon and B.T. Ahn, *Thin Solid Films* **338** (1999) 13.
[7]   F. Adurodija, J. Song, S. K. Kim, K. H. Kang and K. H. Yoon, *Journal of the Korean Physical Society* **32** (1998) 87.
[8]   T. L. Chu, Shirley S. Chu, J. Yue, *Solid-State Science and Technology* **131** (1984) 2182-2185.
[9]   O. Volobujeva, M. Altosaar, J. Raudojaa, E .Mellikov, M. Grossberg, L. Kaupmees, P. Barvinschi, *Solar Energy Materials & Solar Cells* **93** (2009) 11.
[10] S. D. Kim and H. J. Kim, *Journal of the Korean Physical Society* **35** (1999) 403.